SPATIOTEMPORAL ACCURACY GUARANTEE OF POINT CLOUDS FOR URBAN DIGITAL TWIN

Arata Nagasaka[1], Hirohito Ito[2] and Masafumi Nakagawa[3]
[1]Graduate Student, Department of Civil Engineering, Shibaura Institute of Technology
3-7-5, Toyosu, Koto-ku, Tokyo, 135-8548, Japan
Email: mh23025@shibaura-it.ac.jp

[2]Central Consultant Inc
2-5-24, Harumi, Chuo-ku, Tokyo, 104-0053, Japan
Email: hito@central-con.co.jp

[3]Professor, Department of Civil Engineering, Shibaura Institute of Technology
3-7-5, Toyosu, Koto-ku, Tokyo, 135-8548, Japan
Email: mnaka@shibaura-it.ac.jp

KEY WORDS: Digital twin, Accuracy guarantee, Point cloud registration, Spatiotemporal

ABSTRACT: Digital twin is an internet of thing-based concept for solving urban problems. Light detection and ranging (LiDAR) scanners are one of the sensors that acquire shape data in the physical space and are considered suitable for digital twins. However, achieving 100% coverage is difficult by simply installing a small number of fixed sensors within a city, and it is considered effective to integrate information obtained by mobile scanners. By contrast, there are concerns about the reliability of data acquired using mobile scanners, both in terms of time accuracy and location accuracy. Therefore, in this study, we propose a methodology that guarantees the temporal and spatial reliability of mobile scanner data based on fixed scanner data. We conducted an experiment using gait measurement and evaluated accuracy and processing speed. Through qualitative evaluation, we confirmed that spatiotemporal accuracy can be guaranteed in environments with many features, but processing fails in environments with few features. Furthermore, the processing time was approximately 1 Hz. In the future, we plan to improve accuracy, enhance processing speed, and verify the operation using actual robots.

1. INTRODUCTION

The classical digital twin is a concept for solving manufacturing process issues based on a cycle consisting of acquiring physical space information with sensors, recording physical space in digital space, simulating the manufacturing process, and feeding the simulation result back into physical space (Grieves et al., 2017). In recent years, there has been a growing trend of applying this classic digital twin to urban space. By sensing vast urban spaces and applying the digital twin to cities, we can contribute to solving sophisticated social problems. For example, the Tokyo Metropolitan Government in Japan is conducting a demonstration of sensing urban space to provide advanced administrative services in the future. Light detection and ranging (LiDAR) scanners are sensors that can capture the shape of physical space with high precision and are considered suitable for capturing the behavior of cities. However, there are many occlusion in urban spaces, and achieving 100% coverage is difficult by simply installing a small number of LiDAR scanners such as surveillance cameras in cities. Therefore, we thought integrating sensor information obtained by mobile scanners installed in moving vehicles such as self-driving cars (hereinafter, referred to as “probe vehicles”) would be effective. However, sensor information from moving devices has low accuracy in terms of time and location because accurate time synchronization of mobile devices is difficult, GNSS has coverage issues indoors or in obstructed environments, sensors are not designed for high-precision mapping, and position measurement accuracy is also lower than equipment used for civil engineering surveying. In general, to improve simulation accuracy, input data accuracy is required, so to solve advanced social issues with digital twins, acquired data must be highly accurate. Previous studies have shown that large-scale point clouds can be interpolated with mobile scanners (Watanabe, et al., 2014), but applying this methodology to urban environments is difficult because they use markers. Furthermore, in a digital twin, dynamic information and static information may need to be managed separately, as shown in Figure 1. In this case, temporal and spatial consistency between dynamic and static information is required.

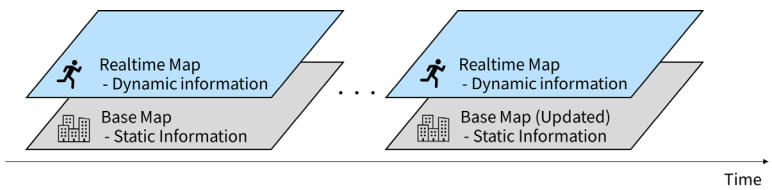

Figure 1. 4D map divided into dynamic and static information for digital twin

While 3D maps are being researched in the field of robotics, there has been little discussion about guaranteeing the temporal accuracy of point clouds and global positional accuracy. In this study, we propose a methodology to guarantee the data accuracy of the time and position of the probe vehicle based on a fixed scanner and generate a time-series map. We show the processing speed, accuracy, and data size for applications in digital twins. In addition, we show changes because of the scanner's scanning pattern.

2. METHODOLOGY

The proposed methodology is shown in Figure 2. First, we acquire time-series point clouds of the same area with a fixed scanner and a mobile scanner. We assume scanners to be installed in autonomous mobile robots and self-driving cars, which we refer to as "probe vehicles" in this work. Next, preprocessing is applied to each point cloud. We identify a moving observer included in the point cloud of a fixed scanner and perform an initial alignment using mobile observer position information identified from the fixed scanners. Following this, correction processing is performed to guarantee spatiotemporal accuracy. Afterward, position accuracy assurance and time accuracy assurance are performed, and subsequently deterministic integration is performed. At this time, time synchronization of the sensor with respect to standard time is required in advance at the network time protocol (NTP) level (approximately 100 ms). In addition, this algorithm requires data collection for several frames before and after to ensure temporal accuracy. At that time, set the threshold for the frames to be verified. As a result, the map whose time position accuracy is guaranteed is updated and can be used for simulation.

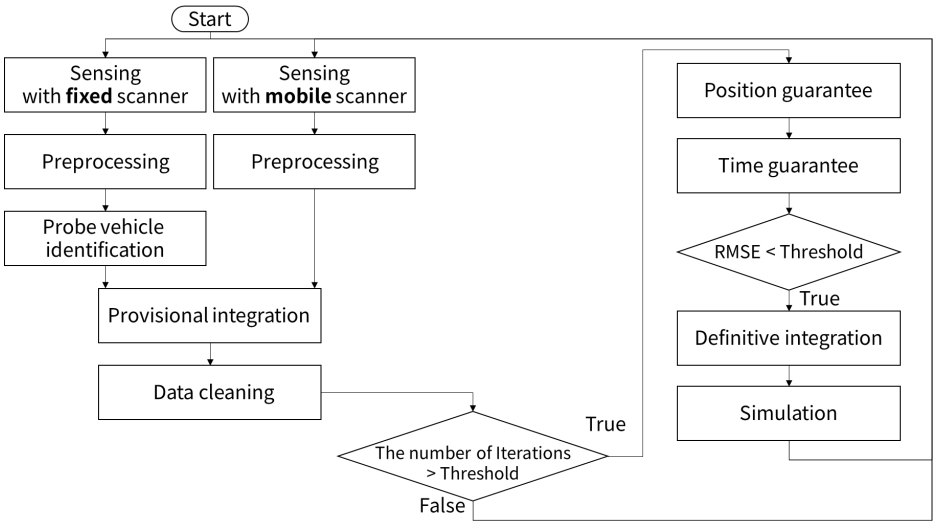

Figure 2. Processing flow overview of the proposed methodology

2.1 Associate Two Scans

Figure 3 shows the preprocessing of a point cloud acquired with a fixed scanner. Assuming that the position of the fixed scanner is obtained using a high-precision positioning method such as RTK-GNSS, the high-precision position information is converted into the Japan plane rectangular coordinate system before being input. The direction of laser irradiation is also measured. Coordinate transformation is performed based on the information of global location and direction. Then, voxelization is performed to obtain a preprocessed point cloud for easier management of the point cloud in the digital twin.

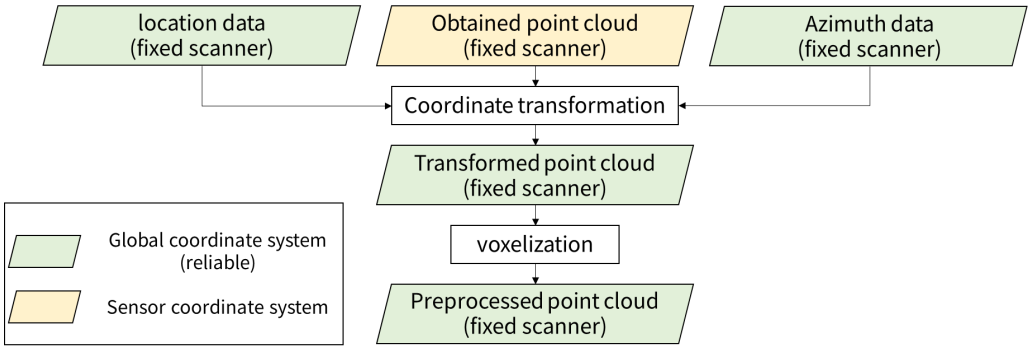

Figure 3. Preprocessing flow of fixed scanner

By contrast, for point clouds acquired with mobile scanners, general point cloud preprocessing such as horizontal correction and removal of distant point clouds is performed to obtain preprocessed point clouds. Then, vehicle identification is obtained. Figure 4 shows the flow of proven vehicle identification. In the probe vehicle identification

process, the difference is first detected by comparing the point cloud acquired from the fixed scanner with the point cloud of the base map. For difference detection, we employ neighborhood search using a KD tree. Next, the point cloud that contains only moving objects is segmented to obtain clusters of moving objects. Then, the probe vehicle reflected in the fixed scanner point cloud is identified, and here we assist in identification using probe vehicle position information. We do not directly use the data from the probe vehicle because the position data obtained from the probe vehicle (for example, using GNSS) may contain errors. Therefore, we employ the process of identifying the probe vehicle from clusters in the point cloud acquired by a fixed scanner.

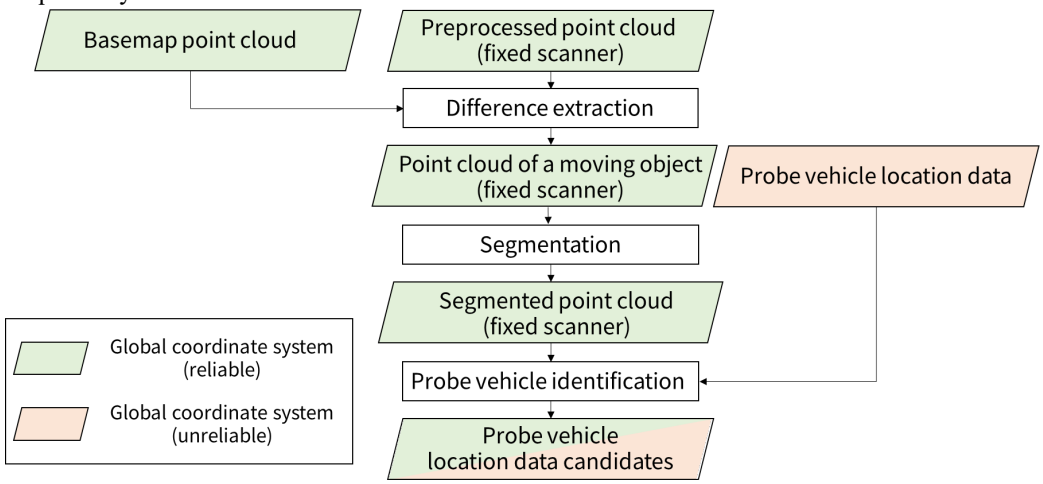

Figure 4. Processing flow of probe vehicle identification

For the initial alignment of the point cloud acquired by the mobile scanner, we use the probe vehicle position data candidates obtained from the probe vehicle identification process. Through this process, candidates for position data of the probe vehicle are obtained. In the correction process, point cloud interpolation and plane estimation are performed. This is because differences in point density and scale affect the accuracy of point cloud registration processing.

2.2 Spatiotemporal Accuracy Guarantee

Positional accuracy is guaranteed by point cloud registration. The algorithm used is generalized iterative closest point (G-ICP), which is expected to improve robustness compared with classical ICP (Segal et al., 2019). Here, point clouds are not merged, but only the coordinate transformation of mobile scanner point clouds is performed. Time accuracy is guaranteed by RMSE calculation of the fixed scanner point cloud and the moving scanner point cloud. Finally, by deterministically integrating each point cloud, the coverage of the map is expanded.

3. EXPERIMENT

The experiment was conducted in the rooftop garden on the 7th floor of the classroom building at Shibaura Institute of Technology Toyosu Campus (Koto-ku, Tokyo, Japan). A noniterative scanning LiDAR scanner (AVIA, Livox) was used for point cloud acquisition from a fixed point, and a noniterative scanning LiDAR scanner (HORIZON, Livox) was used for point cloud acquisition while in motion. The scanning pattern of each scanner was a Lissajous curve. For position acquisition, we applied RTK-GNSS positioning using a GNSS receiver (ZED-F9P, u-blox) and a private GPS-based Control Station at Etchujima Campus of Tokyo University of Marine Science and Technology (Koto-ku, Tokyo). The baseline length was about 800 m. Attitude and heading reference system (AHRS) (MTi-G-710, Xsens) was used for attitude estimation. Table 1 shows the specifications of each sensor, and Figure 6 shows the installation of probe vehicle equipment. Note that there is an offset of approximately 29 cm. This is because preliminary experiments showed that the positioning was not fixed, and previous studies have shown that LiDAR scanners affect GNSS positioning (Meguro et al., 2019).

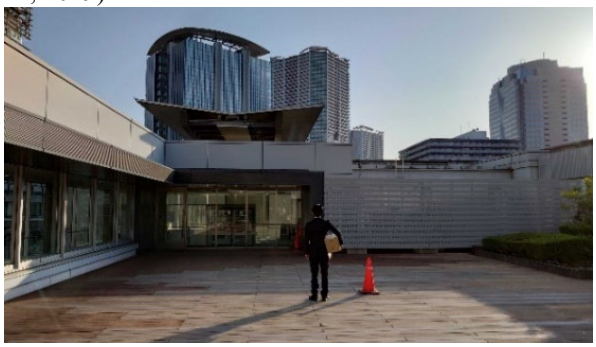

Figure 5. Experiment environment

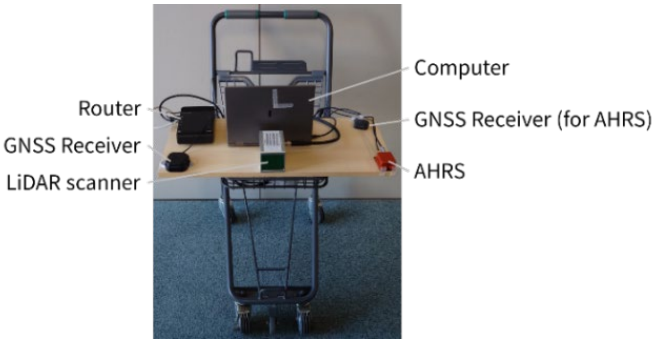

Figure 6. Equipment used (Probe vehicle)

Table1. Sensor specifications

HORIZON (Livox)	
Ranging accuracy	2 cm
Angle measurement accuracy	0.05 °
Ranging range	260 m
FOV (Horizontal × Vertical)	81.7 × 25.1 °
Point cloud acquisition rate	240,000 points / second
AVIA (Livox)	
Range precision	2 cm
Angle measurement accuracy	0.05 °
Detection range	320 m
FOV (Horizontal × Vertical)	70.4 × 77.2 °
Point cloud acquisition rate	240,000 points / second
ZED-F9P (u-blox)	
Positioning accuracy (Horizontal × Vertical)	0.01 / 0.01 cm
Sampling rate	1 Hz
MTi-G-710 (Xsens)	
Angle accuracy	0.2 – 0.8 °
Sampling rate	100 Hz

Table 2 shows the software used. The transformation from the GPS coordinate system to the Japan plane rectangular system was performed using the transformation formula provided by the Geospatial Information Authority of Japan. Because we conducted this experiment in the Tokyo area (not an island area), the coordinate system was the Japan plane rectangular CS IX (EPSG:6677).

Table 2. Software utilized

Software name	Version	Usage
Livox viewer	0.10.0	Point cloud data acquisition
ptpd	2.3.1-debian1-4	Time synchronization between systems
ntpdate	1:4.2.8p12+dfsg-3ubuntu4	Time synchronization with standard time
Livox ROS Driver	V2.6.0	Point cloud file format conversion
MT Manager	2020.0	Posture data acquisition
u-center	22.07	Positioning data acquisition
Matlab	R2020b	Data processing

In the experiment, we synchronized two LiDAR scanners for accurate evaluation. Synchronization was performed by distributing PTPv2 signals within the computer after synchronizing the computer with Japan Standard Time using NTP. In the mobile measurement system, the GNSS receiver and AHRS performed time synchronization using GPS, and the LiDAR scanner used the computer time synchronized with Japanese standard time by NTP, thereby synchronizing the time of the three sensors as shown in Table 3.

Table 3. Time synchronization method

Device name	Synchronization method	Time source
Computer	NTP	NTP server on the internet
HORIZON (Livox)	PTPv2	Computer clock
AVIA (Livox)	PTPv2	Computer clock
ZED-F9P (u-blox)	GPS	GPS satellite
MTi-G-710 (Xsens)	GPS	GPS satellite

4. RESULT

Table 4 shows that initial alignment and data cleaning processing take time. As a result, the overall processing speed was below 2 Hz.

Table 4. Processing time

Processing order	Processing item		processing time [ms]
1 Assume asynchronous	Preprocessing	Fixed scanner	12.4
		Mobile scanner	1.1
2	Probe vehicle identification		95.8
3	Initial alignment and data cleaning		415.7
4	Position guarantee		82.6
5	Time guarantee		5.6
Total			612.1

Figure 7 shows that by differential detection, passersby and probe vehicles can be detected as moving objects that were not present in the base map. By contrast, points and noise that could not be recorded on the base map were also scattered as moving objects.

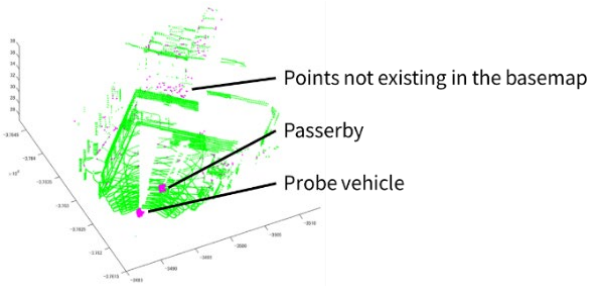

Figure 7. Differential detection result

5. DISCUSSION

First, regarding processing speed, we believe that a speed range of 0.1–10 Hz is necessary, depending on the object of feedback, such as pedestrians and automobiles. As shown in Table 4, it cannot support high request processing speeds. We consider that increasing the speed allows for a wider range of usage scenarios. Regarding the process of initial alignment and data cleaning in Table 4, the interpolation process is inefficient, so changing the processing method can be expected to improve the processing speed. There are existing point group interpolation methods that use image processing in combination, which can also be considered. Next, regarding accuracy evaluation, Table 5 shows the residual evaluation. The most probable values shown in Table 5 are obtained by correcting the measured values because there is an offset of about 29 cm between the GNSS receiver installation position and the LiDAR scanner installation position in the probe vehicle. The estimated value in (1) of Table 5 is the center of gravity of the probe vehicle identified in the probe vehicle identification process. The estimated value in (2) of Table 5 is the position of the center of gravity of the probe vehicle after registration in the position assurance process. This suggests that it is possible to superimpose large-scale point clouds with submeter accuracy using a moving scanner. In terms of performance, we aim for an accuracy of about 10 cm, considering the need to prevent pedestrians from coming into contact with each other, and the technical limitations of sensor accuracy and voxel size. Therefore, we believe that a more accurate superposition is required. Previous papers have shown that registration between occluded and non-occluded point clouds reduces accuracy (Fukutomi et al., 2019). Therefore, by performing registration after detecting occlusion, we can expect to improve accuracy.

Table 5. Residual error to the most probable value

	Residual error [cm]		
	Minimum	Average	Maximum
(1) Identification coordinate value by fixed point scanner	75	80	88
(2) Coordinate values after registration	8	11	17

Table 6 shows that increasing the voxel size reduces the number of point clouds and data size, but it also affects accuracy. In addition, in the best case, it is less than 90%, so improvement is necessary. By contrast, it can be evaluated that there is no significant decrease in accuracy, and there is room for considering the voxel size.

Table 6. Change with voxel size

voxel size	2 cm	5 cm	10 cm
The number of voxels	6394	5683	4264
Time guarantee accuracy rate [%]	84	81	72

In addition, as shown in Figure 8, the accuracy of time accuracy guarantees varies depending on the number of features in the point cloud. It is important to note that the feature values are qualitative evaluations. My interpretation of the graph in Figure 8 is that in scenes with few features, completely incorrect correspondences are made, and in reality, accuracy cannot be guaranteed at all. Therefore, after quantitatively evaluating the features in advance, it is possible to consider an approach that corresponds to a scene with a low concentration of features using linear interpolation and scenes with a high concentration of features before and after.

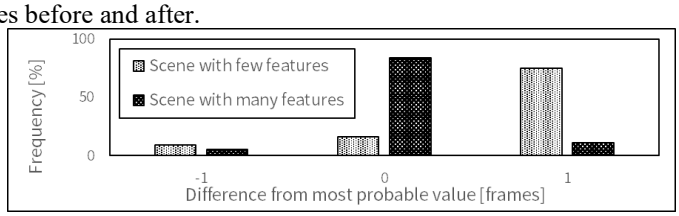

Figure 8. Time accuracy guarantee results

Possible causes of poor accuracy include differences in point density as shown in Figure 9 and the lack of appropriate tie points because of occlusion when images are acquired from different directions. To improve accuracy, we can address occlusion by performing semantic segmentation of moving objects and applying model-based interpolation, while addressing point density differences by interpolating point clouds using image recognition. In this research, we focused on RMSE, but previous research in the field of imaging has shown that it is possible to synchronize multiple cameras using optical flow (Rita et al., 2011). We consider that accuracy can be improved by applying this to point clouds and incorporating processing to track moving objects.

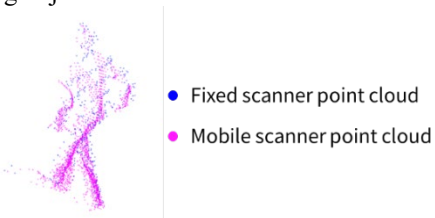

Figure9. Point cloud of a moving object obtained with two scanners

Table 7 shows that RMSE is large, even with position assurance. The RMSE calculated here is not determined using tie points in registration but rather derives from neighboring points of the point group after positional guarantee. Although such calculations separated from the registration process are easy to perform (managing all the metadata derived during the calculation together with the point cloud is difficult), evaluation is difficult in the case of large point clouds. In addition, we consider that RMSE after guaranteeing the position may not be suitable for use as an accuracy index.

Table 7. RMSE after position guarantee

	Minimum	Average	Maximum
RMSE [cm]	47	92	143

In addition, the Livox nonrepetitive scanning (Lissajous curve) LiDAR scanner used in this study can be superimposed over time (Figure 10) compared with repetitive scanning (horizontal linear) LiDAR scanners such as the Velodyne (Figure 11), and the spatial coverage can be improved. When used as a fixed-point scanner, it can faithfully reproduce the urban space, and we consider that it is effective in improving simulation accuracy.

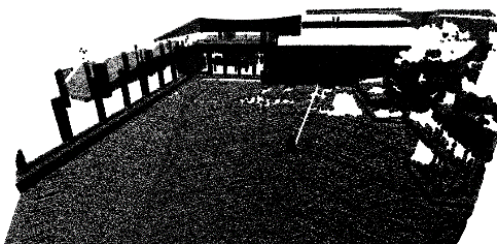

Figure 10. Nonrepetitive scanning

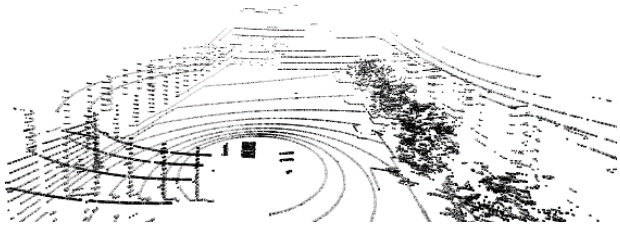

Figure 11. Repetitive scanning

6. CONCLUSION

When applying digital twins to cities, it is required that spatial coverage, real-time performance, and accuracy are guaranteed and that the amount of data is small. Therefore, in this research, we improved spatial coverage by superimposing the fixed scanner point cloud and the mobile scanner point cloud, guaranteed the spatiotemporal accuracy of the mobile scanner using the fixed scanner, and reduced data volume and processing speed by preprocessing. We proposed and verified a method for these improvements. Future prospects include proposing new map update methods, improving processing accuracy and speed, and verifying the reproduction of server and client operations using real robots.

REFERENCES

Fukutomi, D., Maeda, K., Azumi, T., Kato, S., Nishio, N., 2019. The Integration of Two Independent Point Cloud Maps Acquired at Different Times. Embedded Systems Symposium 2019 Proceedings, pp. 54-61.

Grieves, M., Vickers, J., 2017. Digital twin: Mitigating unpredictable, undesirable emergent behavior in complex systems. Transdisciplinary Perspectives on Complex Systems, pp. 85-113

Kawase, K., 2011. A More Concise Method of Calculation for the Coordinate Conversion between Geographic and Plane Rectangular Coordinates on the Gauss-Krüger Projection. GSI journal, 121, pp. 109-124.

Meguro, J., Takeuchi, E., Suzuki, T., 2019. Knowledge of GNSS Failure for Robotics. Journal of the Robotics Society of Japan, Vol. 37 No. 7, pp. 585-592

Segal, A., Haehnel, D., Thrun, S., 2009. Generalized-ICP. Robotics: Science and Systems V, Robotics: Science and Systems Foundation, pp. 435-442.

Rita, T., Tokai, S., Hase, H., 2011. A method of pseudo-synchronization for asynchronous multiple videos. Meeting on Image Recognition and Understanding, pp. 1534-1537.

Watanabe, T., Masuda, H., 2014. Completion of Large-Scale Point-Clouds using Hand-Held 3D Scanners. Proceedings of JSPE Semestrial Meeting, 2014 JSPE Autumn Conference, pp. 389-390.